Hybrid density functional study of armchair SiC nanotubes

Kazi M. Alam and Asok K. Ray*
Department of Physics, University of Texas at Arlington, Arlington, Texas 76019, USA
(Received 22 July 2007; revised manuscript received 8 December 2007; published 29 January 2008)

First-principles calculations for the electronic and geometric structures of *three* different types of armchair silicon carbide nanotubes from (3, 3) to (11, 11) have been performed using hybrid density functional theory and the finite cluster approximation. Full geometry and spin optimizations have been performed without any symmetry constraints. A detailed comparison of the structures and stabilities of the three types of nanotubes is presented. For type 1 nanotube, the cohesive energy appears to saturate at 4.63 eV, whereas for type 2 and 3 nanotubes, the cohesive energy saturates at approximately 4.44 eV. The dependence of the electronic band gaps on the respective tube diameters, energy density of states, and dipole moments as well as Mulliken charge distributions have been investigated. For type 1 nanotubes, Si atoms moved toward the tube axis and C atoms moved in the opposite direction after relaxation, consistent with other SiC nanotubes found in literature. For type 2 and the *newly* proposed type 3, this displacement direction is reversed. The band gaps for type 1 nanotubes are larger than bulk 3*C*-SiC gap, varying between 2.78 and 2.91 eV, while type 2 and type 3 nanotubes have significantly lower band gaps. Unlike the other two types, band gap for type 3 nanotubes decreases monotonically with increasing tube diameter from 1.22 eV for the smallest tube to 0.79 eV for the largest (11, 11) tube studied here. The corresponding numbers for type 2 are 1.49 and 0.91 eV with an oscillatory pattern. None of the tubes appear to be magnetic. It is expected that these tubes will have interesting and important applications in the field of band gap engineering and molecular electronics.

DOI: 10.1103/PhysRevB.77.035436 PACS number(s): 61.48.−c

I. INTRODUCTION

Nanotubes are one of the most studied nanostructures in the current literature. Since the discovery of multiwalled carbon nanotubes (CNT) in 1991,[1] there has been an explosive growth of interest in these kinds of quasi-one-dimensional structures due to their fascinating physical properties and huge potential applications in the electronics industry. Exploring the underlying physics of these structures constitutes the basic building blocks of modern fields of nanoscience and nanotechnology. One distinguishing feature of carbon among other group IV elements in the Periodic Table is that it can participate in either sp^2 or sp^3 bond configurations and can form a variety of phases, such as diamond, graphite, and fullerenes.[2] Single-walled carbon nanotubes have unique characteristics in that they can behave either as metals or semiconductors depending on the tube diameter and chirality. Armchair carbon nanotubes are metallic, while zigzag structures are semiconductors. Length and curvature also play a significant role on structures and energetics.[3–7] Also, carbon-nanotube-based field-effect transistors have advantages over conventional silicon metal-oxide-semiconductor-field-effect transistors such as strong one-dimensional electron confinement, and full depletion in the nanoscale diameter of single-walled carbon nanotubes lead to a suppression of short-channel effects in transistor devices.[8–11] Nanotube-based nonlinear devices can be compact, fast, and sensitive because nanotubes are strong, stable, and uniquely conductive. Researchers have demonstrated that nanotube transistors can have a large current density, high gain, and high carrier mobility.[12–15] Prototype nanotube sensors have demonstrated high sensitivity and detection of electromagnetic and acoustic signals as well as different chemicals.[16–18] Carbon-nanotube-based field-effect transistor, depending on the biasing conditions, can serve as an electrical switch, a light source, and a light detector. Carbon nanotubes provide an ideal model system to study the electrical transport properties of one-dimensional nanostructures and molecules.[19,20]

The extraordinary success in synthesizing and in applications of CNTs has prompted significant experimental and theoretical research on nanostructures of other elements. Group-III nitrides, such as BN, AlN, and GaN, have been synthesized through different techniques.[21–23] Synthesis of several other nanotubes have been reported, for example, NiCl, $H_2Ti_3O_3$, TiO_2, and Si.[24–27] Silicon carbide (SiC) in bulk form is one of the hardest materials and is very suitable for electronic devices designed for operations in extreme environments. In fact, SiC, with its wide band gap, high thermal conductivity, and radiation resistance, is particularly important for use in high-temperature and radiation environments. It is reasonable to assume that the unique properties of bulk SiC, along with properties due to quantum size effects, would also reflect in SiC nanostructures. Indeed, possibilities and promises abound for SiC nanostructures for applications such as nanosensors and nanodevices which can be operated at high temperature, high frequency, and high power. Our group has studied, in detail, the stability of Si_{60} fullerenelike cage by substitutional and endohedral placements of carbon atoms. We found that substitutional carbon doping made the Si_{60} clusters more stable than endohedral doping. Also, stability is higher when the Si and the C atoms are in separate subunits on the cage.[28–30] First-principles calculations based on density functional theory has been performed on the electronic and structural properties of silicon substitutional doping in carbon nanotubes.[31]

Except carbon, group-IV elements have considerable energy differences between sp^2 and sp^3 bonds which suppress the realization of graphitic phase.[32] SiC, in fact, also has a significant energy difference between the sp^2 and sp^3 bonds.

Despite these facts, SiC nanotubes have been successfully synthesized by different groups.[33–41] Sun *et al.*[33] have reported the synthesis of SiC nanotubes through a substitutional reaction with Si atoms replacing half of the C atoms from a multiwalled carbon nanotube. The observed SiC nanotubes were also multiwalled but with higher interplanar spacings than those of multiwalled carbon nanotubes. This indicated weak coupling between inner and outer tubes and possibility of separating them with ease. This motivated us to explore the properties of single wall SiC nanotubes. Indeed, from technological points of view, single-wall nanotubes play more important rolls in molecular electronics. Borowiak-Palen *et al.*[35] produced SiC nanotubes based on high-temperature reactions between silicon powders and multiwalled carbon nanotubes. Hu *et al.*[37] formed SiC nanotubes by reacting CH_4 with SiO. SiC nanotubes are expected to have some advantages over carbon nanotubes. They may possess high reactivity of exterior surface facilitating sidewall decoration and stability at high temperature, harsh environment nanofiber, and nanotube reinforced ceramics.[42] Some *ab initio* methods[43] have shown that the most stable SiC nanotube has the ratio of Si to C of 1: 1. These studies claim that other ratios will eventually collapse the tube into nanowire or clusters with solid interiors. Menon *et al.*[44] have shown that there are two different arrangements (type 1 and type 2) for the most stable SiC nanotubes. They have studied certain nanotubes in armchair and zigzag configuration. Type 1 consists of alternating Si and C atoms with each Si atoms having three C neighbors and vice versa. In type 2 configuration, each Si atom has two C neighbors and one Si neighbor and vice versa. Generalized tight-binding molecular-dynamics and *ab initio* methods were used to study only armchair (6, 6) and zigzag (12, 0). Their calculations revealed that SiC nanotubes with alternating Si and C atoms (type 1) are energetically preferred over the forms that contain C-C and Si-Si bonds (type 2) in addition to Si-C bonds. We propose in this work a *new* type 3 SiC tube which has the same number of Si and C atoms, but differs in the relative spatial positions of Si and C atoms. In this type, each Si has two C and one Si neighbors, has the same constraint as type 2, but Si and C atoms are arranged alternatively in each layer unlike in type 2 where each layer contains either Si or C atoms. So type 3 has one similarity with type 1 in alternating Si and C atoms along one layer perpendicular to the tube axis, though it differs in overall atomic arrangement. As the results below show, type 3 is indeed found to be less stable than types 1 and 2; however, depending on particular applications, type 3 SiC nanotubes can provide an alternate choice. *This study is an ab initio study of the evolution of physical and electronic properties with size (the tube diameter) of three different types of SiC nanotubes of the same helicity*. In particular, in this work, we have studied detailed electronic and geometric structure properties of *three* different types of single wall *armchair* SiC nanotubes from (3, 3) to (11, 11). We have reported the properties of zigzag SiC nanotubes in Ref. 45.

II. COMPUTATIONAL METHOD

Two standard methods in computational condensed matter physics are based on Hartree-Fock (HF) theory and density functional theory (DFT) in the local density approximation or in the generalized gradient approximation. Both methods have their advantages and disadvantages.[46,47] For example, DFT within the local spin density approximation calculations underestimate the band gaps of semiconductors. The discontinuity of exchange-correlation Kohn-Sham potential results in this discrepancy between theoretical and experimental band gaps.[48,49] On the other hand, hybrid density functional theory incorporating HF exchange with DFT exchange-correlation has proved to be an efficient method for many systems. It has been recently verified that hybrid functionals can reproduce the band gaps of semiconductors and insulators quite well.[50,51] In particular, screened hybrid functionals can accurately reproduce band gaps in carbon based materials.[52–55] Thus, in this work, we have opted to use hybrid density functional theory for a detailed step by step investigation of SiC nanotubes. In particular, we have used the B3LYP[56] hybrid functional and the Los Alamos National Laboratory double-ζ basis set[57] as implemented in the GAUSSIAN 03 suite of programs.[58] For silicon atom, the Hay-Wadt pseudopotential[59] and the associated basis set are used for the core and the valence electrons, respectively. For carbon and hydrogen atoms, the Dunning-Huzinaga double-ζ basis set has been employed. Here, we have used finite cluster approach with dangling bonds terminated by hydrogen atoms to simulate the effect of infinite nanotubes. All computations reported here have been performed at the supercomputing facilities of the University of Texas at Arlington.

As mentioned before, we have used the finite cluster-CNT based approach for single wall CNT to construct SiC nanotubes. This approach comprises of rolling a graphenelike sheet of Si and C to form a nanotube. This rolling up can be described in terms of the chiral vector C_h, which connects two sites of the two-dimensional graphenelike sheet that are crystallographically equivalent. This chiral vector maps an atom from the left hand border onto an atom on the right border line and is an integer multiple of the two basis vectors a_1 and a_2, i.e., $C_h = na_1 + ma_2$. So the geometry of any nanotube can be described by the integer pair (n,m) which determines the chiral vector. An armchair nanotube corresponds to the case of $n=m$, and a zigzag nanotube corresponds to the case of $m=0$. All other (n,m) chiral vectors correspond to chiral nanotubes. Here, we are concerned about the armchair nanotube only. As mentioned above, in type 1 arrangement, silicon and carbon atoms are placed alternatively without any adjacent Si or C atoms. In type 2 and type 3 arrangements, the nearest neighbors of each Si atom consist of two C atoms and another Si atom and vice versa. The difference between type 2 and type 3 lies in the relative spatial position of Si and C atoms. If we consider one layer perpendicular to the tube axis, in type 3, Si and C atoms are alternating, while in type 2, each layer contains either Si or C atoms. Figure 1 shows the relative positions of Si and C atoms in all three types of nanotubes, while Figs. 2–4 show the top and side views of (4, 4) and (10, 10) of all three types of nanotubes.

III. RESULTS AND DISCUSSIONS

Table I and Fig. 5 show the variations of the cohesive energies per atom with respect to the total number of Si and

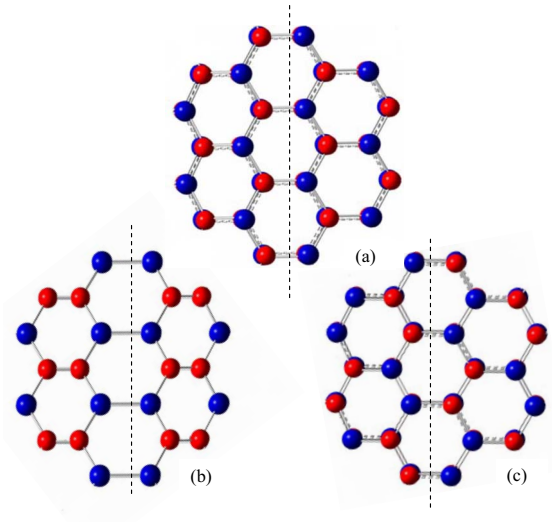

FIG. 1. (Color online) Atomic arrangements for (a) type 1, (b) type 2, and (c) type 3 nanotubes. The carbon atoms are red and silicon atoms are blue. The dashed lines represent the orientation of tube axis.

C atoms for all three types of nanotubes. The cohesive energy or the binding energy per atom for each system was calculated according to the following formula:

$$E_b = \{[aE(\mathrm{Si}) + bE(\mathrm{C}) + cE(\mathrm{H})] - [E(\mathrm{Si}_a\mathrm{C}_b\mathrm{H}_c)]\}/(a+b+c), \quad (1)$$

where a, b, and c are the number of Si, C, and H atoms, respectively. E (Si), E (C), and E (H) are the ground state total energies of Si, C, and H atoms, respectively, and E ($\mathrm{Si}_a\mathrm{C}_b\mathrm{H}_c$) is the total energy of the optimized clusters representing the nanotubes. The default energy convergence criterion was set to 0.0001 a.u. It is evident that type 1 tubes are most stable, while types 2 and 3 have almost the same binding energy. The energy differences are, however, quite small between all three types of armchair SiC nanotubes and *we believe that suitable experimental conditions can design and produce all three types of nanotubes*. As the number of atoms increases, the cohesive energy per atom also increases and approaches saturation. This phenomenon is a common feature for all types of nanotubes. For comparison, the largest type 1 silicon carbide nanotube (SiCNT) studied (11, 11) has a cohesive energy of 4.638 eV/atom, about 67.67% of the bulk (3*C*-SiC) cohesive energy of 6.854 eV/atom. As Si-C bonds are stronger than Si-Si bonds, type 1 nanotubes are more stable than the other two types. The overall symmetry is another reason for their higher binding energies since clusters tend to prefer symmetric structures with higher binding energies.

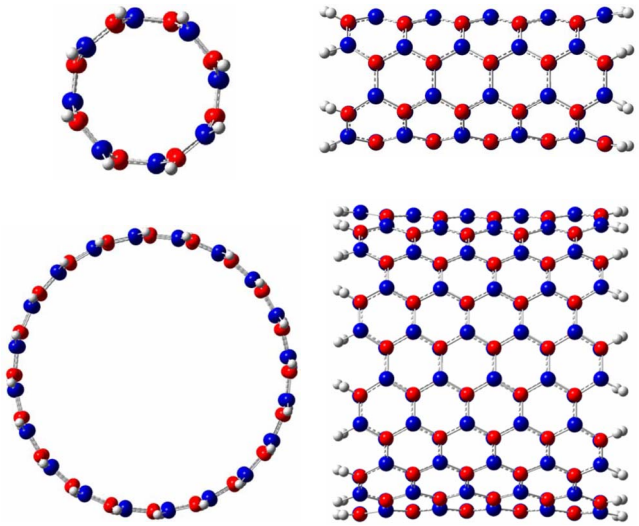

FIG. 2. (Color online) Top and side views of single wall type 1 (4, 4) and (10, 10) SiC nanotubes. Red atoms are carbon and blue atoms are Si.

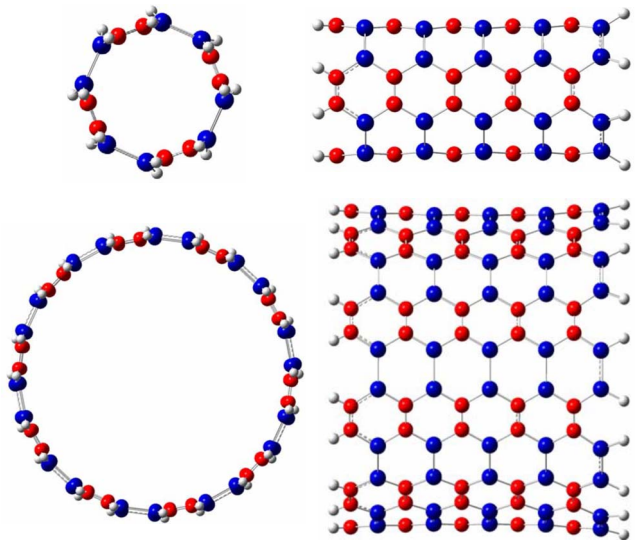

FIG. 3. (Color online) Top and side views of single wall type 2 (4, 4) and (10, 10) SiC nanotubes. Red atoms are carbon and blue atoms are Si.

Table II summarizes the bond length distribution for all nanotubes studied. This bond length distribution rather than

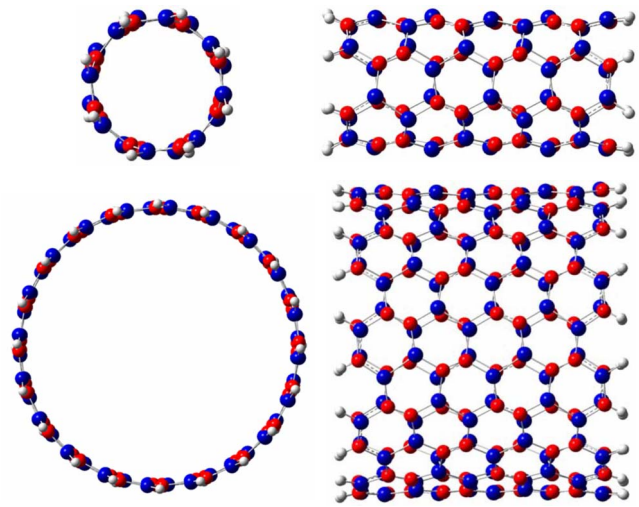

FIG. 4. (Color online) Top and side views of single wall type 3 (4, 4) and (10, 10) SiC nanotubes. Red atoms are carbon and blue atoms are Si.

TABLE I. Cohesive energies/atom (in eV) for armchair SiC nanotubes.

Nanotube	Stoichiometry	Total number of atoms	Cohesive energy per atom (eV)		
			Type 1	Type 2	Type 3
SiC (3, 3)	$Si_{30}C_{30}H_{12}$	72	4.398	4.328	4.228
SiC (4, 4)	$Si_{40}C_{40}H_{16}$	96	4.507	4.344	4.325
SiC (5, 5)	$Si_{50}C_{50}H_{20}$	120	4.560	4.388	4.373
SiC (6, 6)	$Si_{60}C_{60}H_{24}$	144	4.589	4.411	4.399
SiC (7, 7)	$Si_{70}C_{70}H_{28}$	168	4.607	4.425	4.416
SiC (8, 8)	$Si_{80}C_{80}H_{32}$	192	4.619	4.437	4.427
SiC (9, 9)	$Si_{90}C_{90}H_{36}$	216	4.628	4.443	4.435
SiC (10, 10)	$Si_{100}C_{100}H_{40}$	240	4.634	4.448	4.440
SiC (11, 11)	$Si_{110}C_{110}H_{44}$	264	4.638	4.451	4.444

fixed bond length is reminiscent of our *ab initio* calculations performed on hydrogen passivated finite SiC clusters. Generalized tight-binding molecular-dynamics calculations performed on infinite nanotubes usually gives fixed bond lengths unlike *ab initio* calculations. As the diameter or total number of Si and C atoms increase, this bond alteration or the variation range tends to decrease. Tubes of higher curvature with smaller diameter have weaker bonds, resulting in a possible reduction of Young modulus, similar to the cases of C and composite $B_xC_yN_z$ nanotubes.[60] Si-C bond lengths are more widely spread in type 3 than the other two types. This range is narrowest for type 2. On the other hand, Si-Si and C-C bond lengths have more wide range in type 2 than type 3, suggesting possible less electron delocalization in type 2 structures.

After optimization, the nanotube surfaces were found to be slightly rippled. For type 1, more electronegative C atoms moved outward and more electropositive Si moved inward, resulting in two concentric cylinders. This is in good agreement with other *ab initio* results.[42,44,61,62] This surface reconstruction has similar feature observed for group-III nitride nanotubes, where N atoms move away from the tube axis and group-III elements such as Ga, Al, and B move toward the axis.[63–65] For type 2 and type 3 tubes, the average radial distance of Si atoms were higher than that for C atoms, because in those structures in addition to Si-C bonds there are Si-Si and C-C covalent-type bonds. For the latter two cases, this reverse buckling makes the nanotubes Si coated. As mentioned before, Figs. 2–4 show the views of three different types of nanotubes along the axis of symmetry and side views for the armchair configurations. Tight-binding studies[66,67] and Monte Carlo simulations using semiempirical potentials[68] gave an inward displacement of Si and C atoms by relaxation. In contrast to that, one *ab initio* study[69] on 3*C*-SiC surface reported displacements of Si and C atoms into different directions. These radial bucklings caused by bond bending will create surface dipoles and modify the surface band structure, indicating some relevant potential applications of SiC nanotube. Table III shows the average tube diameter and the amount of radial buckling. Type 2 tubes have maximum diameter, followed by type 3 and type 1 nanotubes. The radial buckling has been calculated by subtracting the mean Si radius from the mean C radius (for type 1) and for types 2 and 3, subtracting the mean C radius from

TABLE II. Bond length distributions (in Å) for armchair SiC nanotubes.

Nanotube	Type 1	Type 2			Type 3		
	Si-C (Å)	Si-C (Å)	Si-Si (Å)	C-C (Å)	Si-C (Å)	Si-Si (Å)	C-C (Å)
SiC (3, 3)	1.75–1.83	1.82–1.88	2.25–2.31	1.38–1.43	1.75–1.89	2.25–2.27	1.43–1.45
SiC (4, 4)	1.75–1.82	1.82–1.87	2.24–2.30	1.39–1.45	1.76–1.87	2.23–2.25	1.44–1.45
SiC (5, 5)	1.76–1.82	1.82–1.86	2.23–2.27	1.39–1.45	1.76–1.85	2.23–2.24	1.44–1.45
SiC (6, 6)	1.76–1.81	1.82–1.85	2.25–2.26	1.39–1.44	1.76–1.85	2.22–2.23	1.44–1.46
SiC (7, 7)	1.76–1.81	1.82–1.85	2.24–2.27	1.39–1.45	1.76–1.85	2.22–2.23	1.44–1.46
SiC (8, 8)	1.76–1.82	1.82–1.85	2.23–2.25	1.39–1.45	1.77–1.85	2.22–2.23	1.44–1.46
SiC (9, 9)	1.76–1.81	1.82–1.85	2.23–2.25	1.39–1.45	1.77–1.85	2.22–2.23	1.44–1.46
SiC(10,10)	1.76–1.82	1.82–1.84	2.23–2.25	1.39–1.45	1.77–1.84	2.22–2.23	1.44–1.46
SiC(11,11)	1.76–1.81	1.82–1.84	2.25–2.25	1.39–1.45	1.77–1.85	2.22–2.23	1.44–1.46

TABLE III. Tube diameters (in Å) and radial buckling (in Å) for armchair SiC nanotubes.

	Type 1		Type 2		Type 3	
Nanotube	Tube diameter (Å)	Radial buckling (Å)	Tube diameter (Å)	Radial buckling (Å)	Tube diameter (Å)	Radial buckling (Å)
SiC (3, 3)	5.313	0.037	5.412	0.214	5.375	0.182
SiC (4, 4)	7.022	0.033	7.162	0.202	7.116	0.093
SiC (5, 5)	8.760	0.028	8.936	0.164	8.841	0.071
SiC (6, 6)	10.451	0.023	10.694	0.133	10.582	0.052
SiC (7, 7)	11.786	0.021	12.161	0.115	12.050	0.043
SiC (8, 8)	13.905	0.016	14.240	0.108	14.070	0.035
SiC (9, 9)	15.723	0.013	16.012	0.107	15.816	0.031
SiC (10, 10)	17.351	0.011	17.793	0.092	17.562	0.027
SiC (11, 11)	19.087	0.009	19.576	0.082	19.304	0.022

the mean Si radius. The common feature for all types is that the amount of buckling decreases as the tube diameter increases. This has been shown in Fig. 6. Similar trends were observed for BN nanotubes[60] which has the same arrangement as type 1. However, the amounts of buckling for type 1 nanotubes are smaller than the values found in another *ab initio* calculation.[42] The reason for this difference is attributed to the fact that we have first rolled up the unoptimized graphene SiC sheet and then performed full optimization rather than rolling up the optimized sheet. We believe this is more reasonable since graphene SiC sheets do not exist in nature and because typically in experimental works as mentioned here and reported in the literature, SiC nanotubes were synthesized using carbon nanotubes as templates.[33–41] This difference can also be attributed to different theoretical approaches. Nonetheless, the variation of these bucklings with diameter, namely, the reduction of buckling with diameter increases, well matched with type 1 SiC[42] and BN nanotube cases.[60] The buckling effect is most pronounced in type 2, then type 3 followed by type 1. We need to stress here that the surface reconstruction appears to be a minor effect and might possibly be related to the finite length of the tubes.

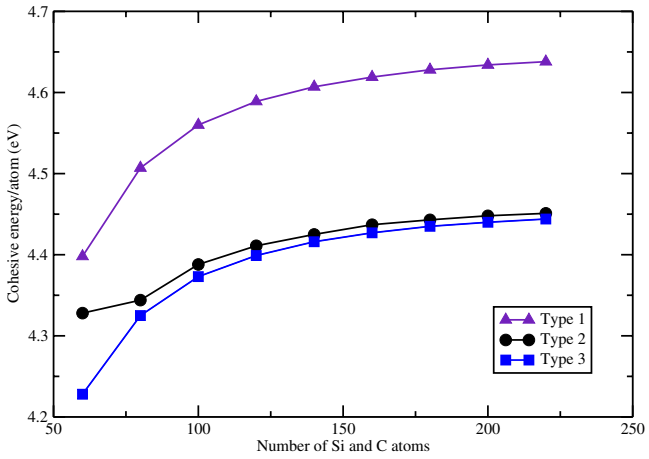

FIG. 5. (Color online) Cohesive energy/atom (eV) vs total number of Si and C atoms.

We also performed Mulliken charge analysis for the nanotubes studied here.[46] All the structures show significant electron transfer from Si to C atoms. Figure 7 implies type 1 armchair structures are more ionic than type 2 and type 3 nanotubes, as they have only Si-C bonds. In fact, the Si-C bonds in type 1 are fully ionic, whereas in type 2 and 3, the bonds, Si-C, Si-Si, and C-C, are a mixture of ionic and covalent bonds. The asymmetry in charge distribution in SiC nanotubes has been and can further be exploited to achieve different electronic properties by exterior-wall decoration at

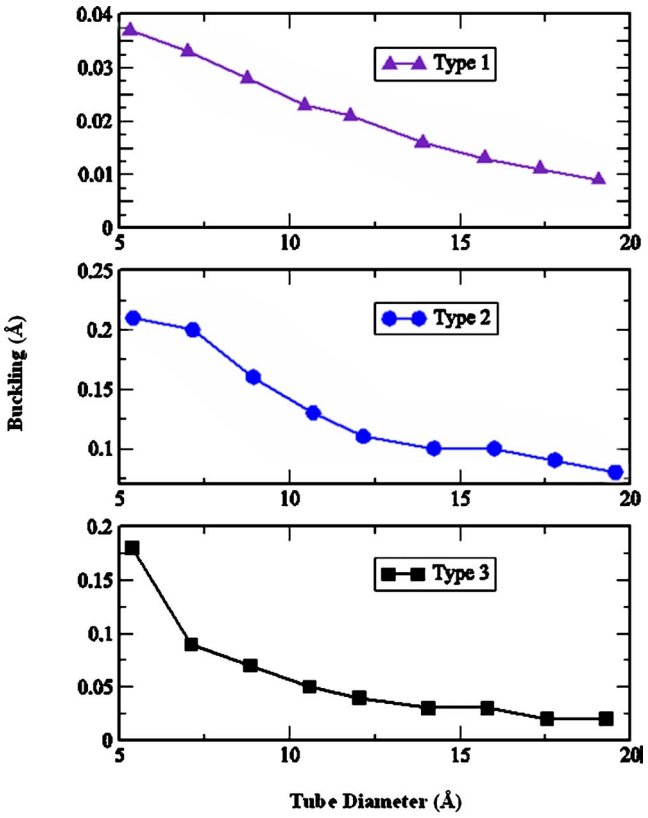

FIG. 6. (Color online) Tube buckling (Å) vs tube diameter (Å) for all three types of SiC nanotubes.

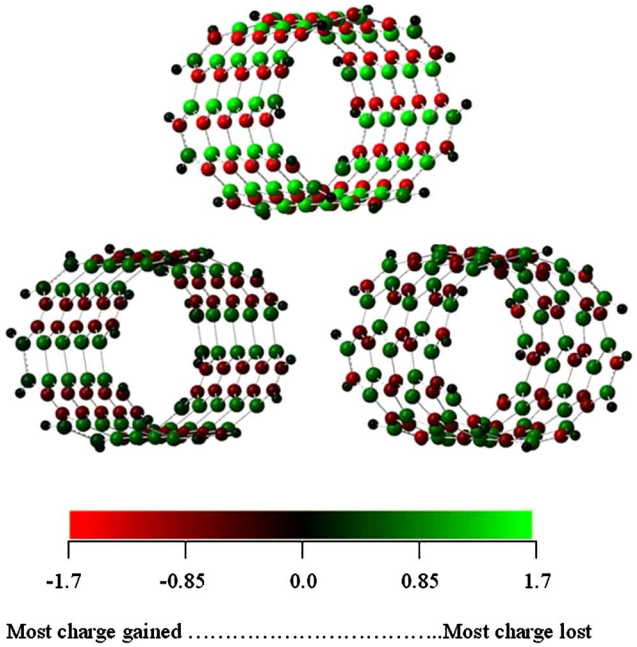

FIG. 7. (Color online) Mulliken charge distributions for (8, 8) nanotubes. Top (type 1), bottom left (type 2) and bottom right (type 3). Carbon atoms gained and silicon atoms lost charge. In case of type 1, maximum amount of charge transfer between Si and C atoms is 1.70*e*. For type 2 and type 3, these values are 0.83*e* and 1.13*e*, respectively.

different adsorption sites.[70,71] This charge transfer is consistent with the radial buckling for type 1 SiCNT as the charge transfer is presumed to occur in one of the C valence orbitals, to which electrons flow from Si atom. The probable existence of more point charges on the wall of type 1 nanotubes might make them better hydrogen storage device than carbon nanotubes[72] and we are indeed pursuing such studies now.[73] However, the same possibilities might also exist for type 2 and 3 nanotubes. Table IV shows the calculated dipole moment for all three types of SiC nanotubes from (3, 3) to (11, 11). Despite the fact that type 1 has ionic bonding between Si and C atoms, the overall dipole moment is low compared to type 2 and type 3 nanotubes. The almost zero dipole moments of type 1 structures indicate an overall highly symmetric charge distribution though all the Si-C bonds are ionic. It is clearly shown that type 3 has slightly higher dipole moment than type 1; thus, it can probably be attributed the same charge symmetry as type 1. In contrast, type 2 structures have significantly higher values which indicate overall charge asymmetry. This fact reveals that symmetric configurations of type 2 nanotubes are characterized by a higher potential energy than the asymmetric configurations, implying that type 2 symmetric nanotubes are less stable than asymmetric type 2 nanotubes. This will have the effect of adherence of type 2 nanotubes into bundles if experimentally synthesized. It is worth noting that type 2 nanotubes have two ends populated by either Si or C atoms. Here, the separations of the positive and negative charges are comparatively large, causing increases in dipole moments. Also, accumulations of charges increase with increases in tube diameters. In type 1 and type 3, the layers perpendicular to the tube axis have alternating C and Si atoms, resulting in low dipole moments. Type 1 nanotubes have almost zero dipole moment due the existence of all perfect hexagons in those structures. In the case of type 3 nanotubes though we do not see any charge polarization, there are two different types of imperfect hexagons, with each having two different orientations. This is the origin of their slightly higher dipole moment than type 1 nanotubes.

TABLE IV. Dipole moments of armchair SiC nanotubes (in Debye).

Nanotube	Type 1 (D)	Type 2 (D)	Type 3 (D)
SiC (3, 3)	0.018	1.242	0.307
SiC (4, 4)	0.001	6.067	0.446
SiC (5, 5)	0.001	7.713	0.226
SiC (6, 6)	0.001	9.767	0.033
SiC (7, 7)	0.050	11.499	0.007
SiC (8, 8)	0.018	13.398	1.311
SiC (9, 9)	0.001	13.337	0.024
SiC (10, 10)	0.000	14.669	0.011
SiC (11, 11)	0.010	16.378	0.371

The highest occupied molecular orbital (HOMO) and the lowest unoccupied molecular orbital (LUMO) gaps give a measure of the "band gap" for the infinite periodic SiC nanotubes. This measure is qualitative in the sense that the tubes studied are finite in length and any extrapolation to infinite tubes should be viewed with caution. After optimization, the lengths of type 1 nanotubes varied from 16.211 to 16.257 Å, with the average length being 16.228 Å. The corresponding numbers for type 2 are 16.014 and 16.346 Å, with the average being 16.297 Å. For type 3, the lengths varied from 16.278 and 16.345 Å, the average being 16.335 Å. The effects of finite size for carbon nanotubes have been studied in detail in the literature[74–77] and we intend to pursue such studies in the future for SiC nanotubes. Table V and Fig. 8 provide the evolution of these gaps as a function of tube diameters for all the structures. The electronic states are also listed in Table V. All the ground state structures we have studied here are in singlet state, i.e., no magnetic structures have been found. The gap is increasing with increasing diameter for type 1 nanotubes and approaching saturation. A slight decreasing trend is observed after (7, 7) but not significant. Type 1 nanotubes have larger band gaps than bulk 3*C*-SiC (2.4 eV). Type 2 and 3 nanotubes have significantly lower gaps. In the case of type 2, gap and tube diameter have an alternating relationship, while for type 3, band gap decreases monotonically with increasing tube diameter and is expected to approach small gap semiconducting to semimetallic regime. These wide ranges of SiC armchair nanotube gaps are in sharp contrast to carbon nanotubes, which are essentially metallic in armchair configuration. Carbon nanotubes are semiconductors in other helicity. The origin of wide band gap for type 1 SiC nanotubes lies in the fact that they have only ioniclike Si-C bonds as compared to the covalent C-C bonds in carbon nanotubes and some Si-Si and C-C

TABLE V. HOMO-LUMO gaps (in eV) and electronic states for armchair SiC nanotubes.

	Type 1 armchair		Type 2 armchair		Type 3 armchair	
SiC Nanotube	HOMO-LUMO gap	Electronic state	HOMO-LUMO gap	Electronic state	HOMO-LUMO gap	Electronic state
SiC (3, 3)	2.776	^1A	1.487	^1A	1.216	^1A
SiC (4, 4)	2.823	^1A	0.806	^1A	1.084	^1A
SiC (5, 5)	2.889	^1A	0.839	^1A	0.905	^1A
SiC (6, 6)	2.932	^1A	0.876	^1A	0.835	^1A
SiC (7, 7)	2.937	^1A	0.727	^1A	0.808	^1A
SiC (8, 8)	2.923	^1A	0.882	^1A	0.799	^1A
SiC (9, 9)	2.919	^1A	0.897	^1A	0.795	^1A
SiC(10, 10)	2.913	^1A	0.905	^1A	0.792	^1A
SiC(11, 11)	2.906	^1A	0.907	^1A	0.791	^1A

bonds in other two types SiC nanotubes in addition to Si-C bonds. More ionic-type bonding localizes the electronic states in type 1 nanotubes and consequently increases the band gap.[42] The band gap variation with tube diameter indicates that type 1 tubes are always wide band gap structures, while type 2 and specifically type 3 tubes are small gap semiconductors and might exhibit metallic behavior. The evolution of band gap with the tube diameter can be analyzed by the curvature induced σ-π hybridization.[35] In the case of type 1 SiC nanotube, as the diameter decreases, curvature increases and the induced σ-π hybridization has the effect of down shifting the conduction bands, resulting in lower gaps with decreasing diameters. For type 3, this trend is reversed in that the curvature induced σ-π hybridization has the effect of uplifting the conduction bands for type 3 structures, resulting in higher band gaps with decreasing diameters. This reverse trend is related to the existence of different bonds in two types of nanotubes. Figure 9 demonstrates energy density of states (DOS) for largest nanotubes (11, 11) in three different configurations. The DOS is built by fitting a Gaussian function in each eigenvalue and then summing them up. The Gaussian width used to broaden the eigenvalues is 0.05 eV and $E=0$ refers to the HOMO. The comparatively large gap of type 1 (11, 11) to the gaps in the other two types is clearly visible.

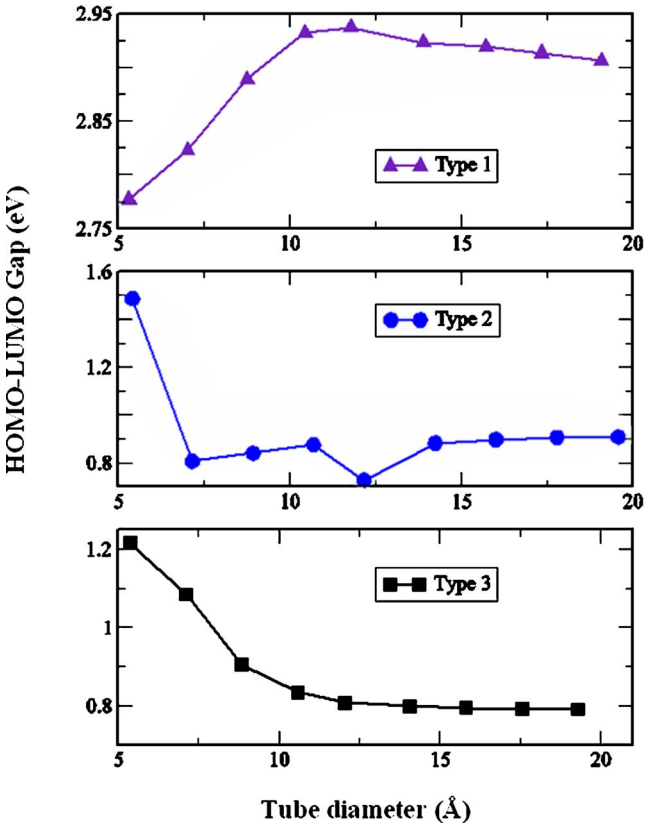

FIG. 8. (Color online) HOMO-LUMO gap (eV) vs tube diameter (Å) for all three types of nanotubes.

Tuning the band gap of semiconductors is an important task and challenging endeavor in molecular electronics as it facilitates the integration of devices and systems for performing a specific work. Among all three types of SiC nanotubes we studied, type 1 which is the most stable one has valence charge density strongly accumulated around C atoms. Significant electron transfer from Si to C atoms results in charge accumulation which makes the nanotube wall highly reactive to the external atom or group of atoms. This asymmetry has been exploited to band structure modification by side wall decoration with H, CH_3, SiH_3, N, NH, NH_2,[70,71,78] and Si or C substitution by N atom.[78] In this work, it has been shown that by changing the relative positions of C and Si atoms, it is possible to have nanotubes with various band gaps. In nanotube-based technology Schottky barriers form at the metal/nanotube junctions, through which carriers must tunnel.[79] These barriers have a profound effect on the function and performance of CNT-based transistors. In general, the charge transfer takes place at the metal nanotube interface leading to band bending and the creation of Schottky barrier.[80] The proposed type 3 single wall SiC armchair nanotube gap is inversely proportional to tube diameter, as is the effective mass, for electrons and holes. Thus, at a given temperature, a larger diameter nanotube will have a larger

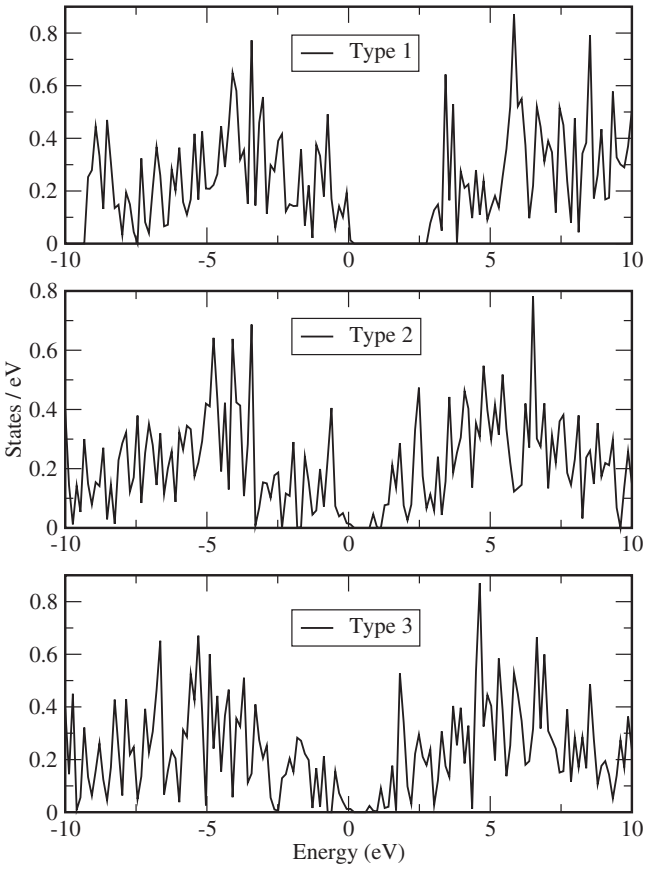

FIG. 9. Density of states for three types of armchair (11, 11) SiC nanotubes. $E=0$ is the HOMO.

free carrier concentration than a smaller diameter nanotube, and they will have a lower effective mass. Consequently, because of the smaller band gap of large diameter nanotubes, the band lineup at the metal/nanotube interface will result in lower Schottky barriers at the transistor source and drain. Tunneling through these barriers will be facilitated because of the smaller effective mass. Though type 2 nanotubes do not show any continuous gap decrease with the increasing diameter, the relationship between HOMO-LUMO gap with the diameter shows they might possess smaller gap at the larger diameters. These indicate that in Si CNT based junctions, type 3 and type 2 might play important role at the nanoscale molecular electronic networks, where SiC nanotubes are desirable over carbon nanotubes for some specific reasons. For example, one of the limitations of CNTs is their inability to survive in high-temperature, harsh-environment applications. Silicon carbide nanotubes are preferred for their superior material properties under such conditions.

IV. CONCLUSIONS

We have studied three different types of single wall SiC nanotubes in armchair configuration. Detailed analysis and comparison for stability and geometry have been performed along with the evolution of electronic properties with the tube diameters. Within the same helicity and under the constraint of Si to C ratio as 1:1, the dominant factor in deciding the stability, tube morphology, and electronic behavior is the relative position of Si and C atoms, and consequently, the nature of chemical bonds. As the number of atoms increases, the cohesive energy of nanotubes increases and approaches saturation. This is a common feature for all types of nanotubes. Three armchair nanotubes are close in energy, with type 1 predicted to be most stable. Slight difference in hybridization of Si and C atoms on the tube surface causes radial buckling and surface dipoles forming from these bucklings may have potential applications at the nanoscale regime. The Mulliken charge analysis shows that type 1 structures are more ionic than type 2 and 3 structures. Unlike carbon nanotubes which are metallic in armchair configuration, all three types of SiC nanotubes are semiconductors, where type 1 tubes have the largest band gaps. Strong ionic-type bonding localizes the electronic states which results in wide band gap for the type 1 nanotubes. Type 2 and 3 nanotubes have significantly lower gaps. While type 2 nanotubes exhibit a zigzag type trend in gap and diameter relationship, there is a monotonous decrease in band gap with increasing tube diameter for type 3. The smaller band gaps of type 2 and type 3 armchair SiC nanotubes with larger diameters can open a new road to reduce Schottky barrier at the nanotube metal junction. These two types might even exhibit metallic behavior at higher diameter. Our binding energy calculations reveal that all three types of armchair nanotubes are stable and close in energy. Thus, if they are synthesized under suitable environment, one can envision all-nanotube electronics based on SiC nanotubes, where metallic and semiconducting tubes would form high current carrying conductors and active devices respectively.

ACKNOWLEDGMENTS

The authors gratefully acknowledge partial support from the Welch Foundation, Houston, Texas (Grant No. Y-1525). Also, helpful discussions with R. Atta-Fynn are acknowledged.

*akr@uta.edu

[1] S. Iijima, Nature (London) **354**, 56 (1991); S. Iijima and T. Ichihashi, *ibid.* **363**, 603 (1993).

[2] *Carbon Nanotubes-Synthesis, Structure, Properties and Applications*, Topics in Applied Physics Vol. 80, edited by M. S. Dresselhaus, G. Dresselhaus, and Ph. Avouris (Springer, Berlin, 2001).

[3] N. Hamada, S. I. Sawada, and A. Oshiyama, Phys. Rev. Lett. **68**, 1579 (1992).

[4] R. Saito, M. Fujiata, G. Dresselhaus, and M. S. Dresselhaus, Appl. Phys. Lett. **60**, 2204 (1992).

[5] T. W. Odom, J. L. Huang, P. Kim, and C. M. Lieber, Nature

(London) **391**, 62 (1998).
[6] R. A. Jishi, J. Bragin, and L. Lou, Phys. Rev. B **59**, 9862 (1999).
[7] O. Gulseren, T. Yildirim, and S. Ciraci, Phys. Rev. B **65**, 153405 (2002).
[8] S. Wind, J. Appenzeller, R. Martel, V. Derycke, and Ph. Avouris, Appl. Phys. Lett. **80**, 3817 (2002).
[9] Javey, J. Guo, Q. Wang, M. Lundstrom, and H. Dai, Nature (London) **427**, 654 (2003).
[10] J. Appenzeller, Y. M. Lin, J. Knoch, Z. Chen, and P. Avouris, IEEE Trans. Electron Devices **52**, 2568 (2005).
[11] J. Guo, M. Lundstrom, and S. Datta, Appl. Phys. Lett. **80**, 3192 (2002).
[12] W. A. de Heer, A. Chatelain, and D. Ugarte, Science **270**, 1179 (1995).
[13] W. Zhu, C. Bower, O. Zhou, G. Kochanski, and S. Jin, Appl. Phys. Lett. **75**, 873 (1999).
[14] C. Bower, D. Shalóm, W. Zhu, D. López, G. P. Kochanski, P. L. Gammel, and S. Jin, IEEE Trans. Electron Devices **49**, 1478 (2002).
[15] T. Durkop, S. A. Getty, E. Cobas, and M. S. Fuhrer, Nano Lett. **4**, 35 (2004).
[16] J. Suehiro, G. Zhou, and M. Hara, Sens. Actuators B **105**, 164 (2005).
[17] M. Penza, G. Cassano, P. Aversa, A. Cusano, A. Cutolo, M. Giordano, and L. Nicolais, Nanotechnology **16**, 2536 (2005).
[18] J. Kong, N. Franklin, C. Zhou, S. Peng, J. J. Cho, and H. Dai, Science **287**, 622 (2000).
[19] S. J. Wind, J. Appenzeller, and P. Avouris, Phys. Rev. Lett. **91**, 058301 (2003).
[20] A. Javey, J. Guo, M. Paulsson, Q. Wang, D. Mann, M. Lundstrom, and H. Dai, Phys. Rev. Lett. **92**, 106804 (2004).
[21] J. Cumings and A. Zettl, Chem. Phys. Lett. **316**, 211 (2000).
[22] Q. Wu, Z. Hu, X. Wang, Y. Lu, X. Chen, H. Xu, and Y. Chen, J. Am. Chem. Soc. **125**, 10176 (2003).
[23] J. Goldberger, R. He, Y. Zhang, S. Lee, H. Yan, H. Chol, and P. Yang, Nature (London) **422**, 599 (2003).
[24] Y. R. Hacohen, E. Grunbaum, R. Tenne, J. Sloand, and J. L. Hutchinson, Nature (London) **395**, 336 (1998); Y. R. Hacohen, R. Popovitz-Biro, E. Grunbaum, Y. Prior, and R. Tenne, Adv. Mater. (Weinheim, Ger.) **14**, 1075 (2002).
[25] Q. Chen, W. Zhou, G. Du, and L. M. Peng, Adv. Mater. (Weinheim, Ger.) **14**, 1208 (2002).
[26] G. R. Patzke, F. Krumeich, and R. Nesper, Angew. Chem., Int. Ed. **41**, 2446 (2002).
[27] J. Sha, J. Niu, X. Ma, J. Xu, X. Zhang, Q. Yang, and D. Yang, Adv. Mater. (Weinheim, Ger.) **14**, 1219 (2002).
[28] A. Srinivasan, M. N. Huda, and A. K. Ray, Phys. Rev. A **72**, 063201 (2005).
[29] M. N. Huda and A. K. Ray, Phys. Rev. A **69**, 011201(R) (2004); A. K. Ray and M. N. Huda, J. Comput. Theor. Nanosci. **3**, 315 (2006) and references therein.
[30] M. N. Huda, L. Kleinman, and A. K. Ray, J. Comput. Theor. Nanosci. **4**, 739 (2007).
[31] R. J. Baierle, S. B. Fagan, R. Mota, A. J. R. da Silva, and A. Fazzio, Phys. Rev. B **64**, 085413 (2001).
[32] M. T. Yin and M. L. Cohen, Phys. Rev. B **29**, 6996 (1984).
[33] X. H. Sun, C. P. Li, W. K. Wong, N. B. Wong, C. S. Lee, S. T. Lee, and B. T. Teo, J. Am. Chem. Soc. **124**, 14464 (2002).
[34] N. Keller, C. Pham-Huu, G. Ehret, V. Keller, and M. J. Ledous, Carbon **41**, 2131 (2003).
[35] E. Borowiak-Palen, M. H. Ruemmeli, T. Gemming, M. Knupfer, K. Biedermann, A. Leonhardt, T. Pihler, and R. J. Kalenczuk, J. Appl. Phys. **97**, 056102 (2005).
[36] T. Taguchi, N. Igawa, H. Yamamoto, S. Shamoto, and S. Jitsukawa, Physica E (Amsterdam) **28**, 431 (2005).
[37] J. Q. Hu, Y. Bando, J. H. Zhan, and D. Goberg, Appl. Phys. Lett. **85**, 2923 (2004).
[38] J. M. Nhut, R. Vieira, L. Pesant, J.-P. Tessonnier, N. Keller, G. Ehet, C. Pham-Huu, and M. J. Ledoux, Catal. Today **79**, 11 (2002).
[39] C. Pham-Huu, N. Keller, and G. Ehet, J. Catal. **200**, 400 (2001).
[40] T. Taguchi, N. Igawa, H. Yamamoto, and S. Jitsukawa, J. Am. Ceram. Soc. **88**, 459 (2005).
[41] A. Huczko, M. Bystrzejewski, H. Lange, A. Fabianowska, S. Cudzilo, A. Panas, and M. Szala, J. Phys. Chem. B **109**, 16244 (2005).
[42] M. W. Zhao, Y. Y. Xia, F. Li, R. Q. Zhang, and S.-T. Lee, Phys. Rev. B **71**, 085312 (2005).
[43] G. Mavrandonakis, E. Froudakis, M. Schnell, and M. Muhlhä, Nano Lett. **3**, 1481 (2003).
[44] M. Menon, E. Richter, A. Mavrandonakis, G. Froudakis, and A. N. Andriotis, Phys. Rev. B **69**, 115322 (2004).
[45] K. Alam and A. K. Ray, Nanotechnology **18**, 495706 (2007).
[46] W. J. Hehre, L. Radom, P. v. R. Schleyer, and J. A. Pople, *Ab Initio Molecular Orbital Theory* (Wiley, New York, 1986); D. C. Young, *Computational Chemistry* (Wiley, New York, 2001).
[47] P. Hohenberg and W. Kohn, Phys. Rev. **136**, B864 (1964); W. Kohn and L. J. Sham, Phys. Rev. **140**, A1133 (1965); D. M. Ceperley and B. J. Alder, Phys. Rev. Lett. **45**, 566 (1980); J. C. Slater, *The Self Consistent-Field for Molecules and Solids*, Quantum Theory of Molecules and Solids Vol. 4 (McGraw-Hill, New York, 1974); S. H. Vosko, L. Wilk, and M. Nusair, Can. J. Phys. **58**, 1200 (1980); R. G. Parr and W. Yang, *Density Functional Theory of Atoms and Molecules* (Oxford University Press, New York, 1989).
[48] J. P. Perdew, R. G. Parr, M. Levy, and J. L. Balduz, Phys. Rev. Lett. **49**, 1691 (1982).
[49] J. P. Perdew and M. Levy, Phys. Rev. Lett. **51**, 1884 (1983).
[50] J. Muscat, A. Wander, and N. Harrison, Chem. Phys. Lett. **34**, 397 (2001).
[51] J. Heyd and G. Scuseria, J. Chem. Phys. **121**, 1187 (2004).
[52] V. Barone, J. E. Peralta, M. Wert, J. Heyd, and G. E. Scuseria, Nano Lett. **5**, 1621 (2005).
[53] V. Barone, J. E. Peralta, and G. E. Scuseria, Nano Lett. **5**, 1830 (2005).
[54] V. Barone, O. Hod, and G. E. Scuseria, Nano Lett. **6**, 2748 (2006).
[55] M. Y. Han, B. Ozyilmaz, Y. Zhang, and P. Kim, Phys. Rev. Lett. **98**, 206805 (2007).
[56] A. D. Becke, J. Chem. Phys. **98**, 5648 (1993); **109**, 2092 (1998); C. Lee, W. Yang, and R. G. Parr, Phys. Rev. B **37**, 785 (1988).
[57] T. H. Dunning, Jr. and P. J. Hay, *Modern Theoretical Chemistry* (Plenum, New York, 1976), pp. 1–28.
[58] M. J. Frisch, G. W. Trucks, H. B. Schlegel, G. E. Scuseria, M. A. Robb, J. R. Cheeseman, J. A. Montgomery, Jr., T. Vreven, K. N. Kudin, J. C. Burant, J. M. Millam, S. S. Iyengar, J. Tomasi, V. Barone, B. Mennucci, M. Cossi, G. Scalmani, N. Rega, G. A. Petersson, H. Nakatsuji, M. Hada, M. Ehara, K. Toyota, R. Fukuda, J. Hasegawa, M. Ishida, T. Nakajima, Y. Honda, O. Kitao, H. Nakai, M. Klene, X. Li, J. E. Knox, H. P. Hratchian, J.

B. Cross, C. Adamo, J. Jaramillo, R. Gomperts, R. E. Stratmann, O. Yazyev, A. J. Austin, R. Cammi, C. Pomelli, J. W. Ochterski, P. Y. Ayala, K. Morokuma, G. A. Voth, P. Salvador, J. J. Dannenberg, V. G. Zakrzewski, S. Dapprich, A. D. Daniels, M. C. Strain, O. Farkas, D. K. Malick, A. D. Rabuck, K. Raghavachari, J. B. Foresman, J. V. Ortiz, Q. Cui, A. G. Baboul, S. Clifford, J. Cioslowski, B. B. Stefanov, G. Liu, A. Liashenko, P. Piskorz, I. Komaromi, R. L. Martin, D. J. Fox, T. Keith, M. A. Al-Laham, C. Y. Peng, A. Nanayakkara, M. Challacombe, P. M. W. Gill, B. Johnson, W. Chen, M. W. Wong, C. Gonzalez, and J. A. Pople, GAUSSIAN 03, Revision A.1, Gaussian Inc. Pittsburgh, PA, 2003.

[59] P. J. Hay and W. R. Wadt, J. Chem. Phys. **82**, 270 (1995).

[60] E. Hernandez, C. Goze, P. Bernier, and A. Rubio, Phys. Rev. Lett. **80**, 4502 (1998).

[61] R. J. Baierle, P. Piquini, L. P. Neves, and R. H. Miwa, Phys. Rev. B **74**, 155425 (2006).

[62] Y. Miyamoto and B. D. Yu, Appl. Phys. Lett. **80**, 586 (2002).

[63] M. W. Zhao, Y. Y. Xia, D. J. Zhang, and L. M. Mei, Phys. Rev. B **68**, 235415 (2003).

[64] S. M. Lee, Y. H. Lee, Y. G. Hwang, J. Elsner, D. Porezag, and Th. Frauenheim, Phys. Rev. B **60**, 7788 (1999).

[65] M. Menon and D. Srivastava, Chem. Phys. Lett. **307**, 407 (1999).

[66] S. P. Mehandru and A. B. Anderson, Phys. Rev. B **42**, 9040 (1990).

[67] D. H. Lee and J. D. Joannopoulos, J. Vac. Sci. Technol. **21**, 351 (1982).

[68] T. Takai, T. Halicioglu, and W. A. Tiller, Surf. Sci. **164**, 341 (1985).

[69] B. Wenzien, P. Käckell, and F. Bechstedt, Surf. Sci. **308-309**, 989 (1994).

[70] M. W. Zhao, Y. Y. Xia, R. Q. Zhang, and S.-T. Lee, J. Chem. Phys. **122**, 214707 (2005).

[71] F. Li, Y. Y. Xia, M. W. Zhao, X. D. Liu, B. D. Huang, Z. H. Yang, Y. J. Ji, and C. Song, J. Appl. Phys. **97**, 104311 (2005).

[72] G. Mpourmpakis, G. E. Froudakis, G. P. Lithoxoos, and J. Samios, Nano Lett. **6**, 1581 (2006).

[73] S. Mukherjee and A. K. Ray, J. Comp. Th. Nanosci. (to be published).

[74] R. Saito, T. Takeya, T. Kimura, G. Dresselhaus, and M. S. Dresselhaus, Phys. Rev. B **59**, 2388 (1999).

[75] J. Wu, W. Duan, B.-L. Gu, J.-Z. Yu, and Y. Kawazoe, Appl. Phys. Lett. **77**, 2554 (2000).

[76] R. B. Chen, C. P. Chang, F. L. Shyu, J. S. Hwang, and M. F. Lin, Carbon **42**, 531 (2004).

[77] O. Hod, J. E. Peralta, and G. E. Scuseria, arXiv:physics/0609091 (unpublished).

[78] T. He, M. Zhao, Y. Xia, W. Li, C. Song, X. Lin, X. Liu, and L. Mei, J. Chem. Phys. **125**, 194710 (2006).

[79] F. Leonard and J. Terso, Phys. Rev. Lett. **83**, 5174 (1999).

[80] S. M. Sze, *Physics of Semiconductor Devices*, 2nd ed. (Wiley, 1981).